THE UNIVERSITY *of* EDINBURGH
School of Physics
and Astronomy

Senior Honours Project

Nuclear Transparency of $1\pi 1$nucleon Events from 2.26GeV Electron-Carbon Scattering

Jan Kocka
31th of March 2023

Abstract

We outline the need for a better understanding of neutrino-nucleus interactions and how studying electron-nucleus interaction can be used for the purpose. It covers some of the prerequisites to understand such studies, including the most commonly studied interaction types and the use of Monte Carlo event generators like GENIE. An introduction to the CLAS6 data used by the e4ν collaboration is presented and a new codebase using modern C++ to analyse the data was developed. Finally we use this code to conduct a study of nuclear effects on the reconstruction of pion momentum of 1 pion 1 nucleon events (mainly from Δ_{1232} resonances) from GENIE generated 2.26GeV incident electron - carbon nucleus scattering. We identify errors of the reconstruction due to initial state effects and final state interactions, and show that even when accounting for detector precision such reconstruction may be possible to within a 400 Mev/c bin.

Declaration

I declare that this project and report is my own work.

Acknowledgements

I would like to thank my supervisor Cheryl Patrick for always being very welcoming and helpful with my many questions, and her patience throughout the project. I would also like to thank Steven Dytman for further help guiding the project and the physics of the project.

Supervisor: Dr. Cheryl Patrick

Date: 31/3/2023
Completed in 10 Weeks

Contents

1 Neutrino Oscillations and Understanding Neutrino Scattering

This project concerns neutrinos and their properties, and so a brief description of the relevant properties and their scientific significance is presented. Neutrinos are three uncharged leptons of different flavours (each corresponding to the other 3, charged, leptons – electron, μ and τ of ascending masses). Neutrinos interact only via the weak force and with very low cross sections, the Feynman diagrams of their interactions with the other fundamental particles through the W and Z bosons are shown in fig. 1.

Their existence was originally proposed by Pauli in the 1930s to explain the beta decay, and their mass was long thought to be zero, most notably the standard model assumes this. However at the end of the last century neutrinos have been observed to undergo oscillations which implies non-zero mass. Since then they have been at the forefront of research, nowadays they are generally accepted to have mass and there are questions about them being their own antiparticles (Majorana) and possibly violating charge-parity symmetry. The answers to these questions could significantly further our understanding of the universe, including explaining the dominance of matter over antimatter.

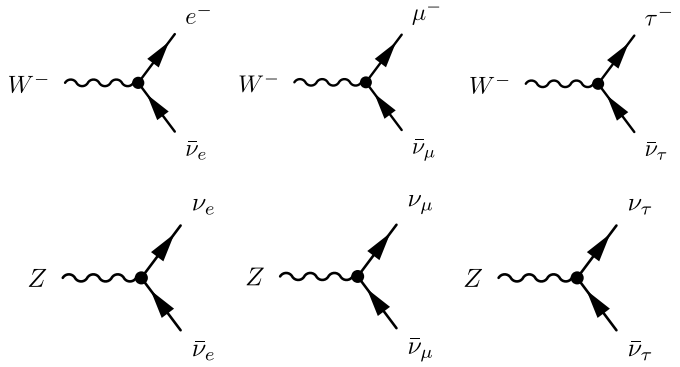

Figure 1: Feynman diagrams of weak force vertices for neutrino interactions, all other vertices including them can be obtain by suitable rotations of these (this requires replacing some particles with their antiparticles, including the W^-becoming a W^+). Say the first could be changed to represent a e^- and W^+ colliding and forming a ν_e. Diagrams taken from [1].

1.1 Neutrino oscillations

In particle physics oscillations is a phenomenon that takes place when the particle mass eigenstates which govern its evolution in time are not the same as the states in which it can be observed. This phenomenon is not exclusive to neutrinos, the neutral Kaon has been known to oscillate to its own antiparticle and vice-versa since before neutrino oscillations were discovered [2].

In the case of neutrinos, we say there are three flavour states and the way we differentiate them is by the weak interaction as so far all observed interactions conserve the three separate lepton numbers (electron, μ and τ again). So say an electron capture takes place when an electron interacts with a proton to form a neutron and a neutrino, then we observe that neutrino to be an electron neutrino in order to conserve the electron lepton

number and we can say it is collapsed into the electron neutrino eigenstate.

Further, that electron eigenstate can be expressed in terms of the mass eigenstates, and if the two eigenstate sets aren't identical it will have multiple non-zero components. Then as the mass eigenstates travel differently (the neutrino has a definite E and so through $E^2 = m^2 + p^2$ we get that the mass eigenstates have different momenta and so speeds), the relative components of the state at different positions as it travels will change periodically – oscillate. Thus the probabilities of measuring the neutrino in any of the three flavour states also oscillates.

A very important property resulting from the two eigenstate sets being different is the transformation matrix between them. For neutrinos this is the PMNS[1] matrix, it is referred to as U and is such that

$$|\nu_\alpha\rangle = \sum_i U_{\alpha i} |\nu_i\rangle \,, \text{ and } |\nu_i\rangle = \sum_\alpha U^\dagger_{i\alpha} |\nu_\alpha\rangle \tag{1}$$

where $|\nu_\alpha\rangle$ are the three flavour eigenstates and $|\nu_i\rangle$ the mass eigenstates. The exact form of the matrix then determines many of the neutrino properties, obtaining accurate values for its elements is the main driving force of neutrino oscillation experiments. For example if the matrix is not completely real then neutrinos violate CP symmetry[3].

Then to complete the picture, the probability of a neutrino measured to be of flavour α, to be measured again in flavour β is given by

$$P(\alpha \to \beta) = \sum_i |U_{\alpha i} U^\dagger_{i\beta}|^2 + 2\,\mathrm{Re} \sum_{j>i} U_{\alpha i} U^\dagger_{i\beta} (U_{\alpha j} U^\dagger_{j\beta})^* \exp\left(-i \frac{\Delta m^2_{ij}}{2} \frac{L}{E}\right) \tag{2}$$

where E is it's energy, L the distance between our measurements and Δm^2_{ij} the mass difference of the mass eigenstates i, j squared (for more detail see [3]). This is then our main entry point for studying the PMNS matrix from oscillation experiments as we can measure these probabilities P and so get insight into the $U_{\alpha i}$ elements along with the mass differences Δm_{ij}. Though notably, even if we knew precisely all the oscillation probabilities we would not have all the information to fully determine U as there may be Majorana phase components that doesn't influence P, these need to be studied by other experiments like neutrinoless β decay [4].

1.2 Oscillation experiments and energy reconstruction

There are many active experiments (NOvA[5] and T2K[6] currently running and DUNE[7] and Hyper-Kamiokande[8] under development) working on precise neutrino oscillation measurements to determine the neutrino masses and PMNS matrix elements. In these (long-baseline) experiments, neutrinos from a source which has known fractions of the three flavours are beamed across large distances (for oscillations of $\sim$ 1GeV ν_μ an L of order $\sim$ 1000km is needed [9]) so that they oscillate and then some of the flavours (electron, μ or both) are observed and counted. This means we are measuring some of the probabilities from eq. (2) with a known L, however we don't have a simple value for E which we need in order to interpret the data. Experiments typically use either neutrinos

[1]Stands for Pontecorvo–Maki–Nakagawa–Sakata matrix, it is the analogue of the CKM matrix for the mixing of quarks.

from the sun, from the atmosphere due to the cosmic microwave background or from secondary neutrino beams at accelerators and all of these methods produce neutrinos with wide ranges of energies (see fig. 2). Because of that experiments rely on reconstructing incident neutrino energies and for that a very good understanding of the detecting mechanism is needed.

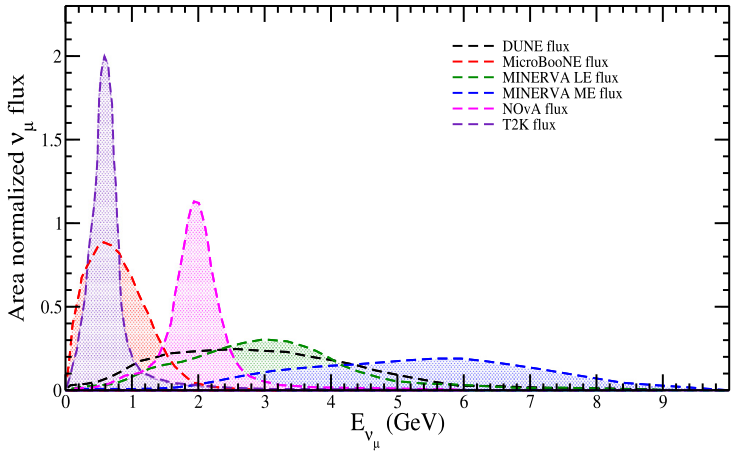

Figure 2: The energy distributions of neutrino sources used at various experiments, both oscillation (DUNE, NOvA, T2K) and neutrino interaction studies (MicroBooNE[10], MINERVA[11]). All of these are accelerator based sources which have the narrowest energy distributions, however still the spread is on the order of hundreds of MeV at least. Figure taken from [12].

As neutrinos are uncharged and have tiny cross sections, they aren't detected directly, instead a large amount of some stable substance (argon, water or chlorine) is stored and surrounded by detectors (Cherenkov detectors, plastic/carbon based scintillators). Then when neutrinos come in, some will interact with these atoms and produce detectable particles. These always have to include a lepton of the corresponding flavour and possibly other particles, often nucleons, photons or pions and a collection of particle measurements originating from one neutrino is called an event. While the neutrinos can interact with the atomic electrons [13], it is only significant at low neutrino energies and rarely relevant to oscillation experiments. Thus some of the most important physics of neutrino detectors are the neutrino-nucleus interactions and these are not yet well understood. Modern oscillation experiments report these limitations to be a source of large systematic uncertainties[14, 15].

1.3 e4ν and nuclear effects

Which is where e4ν comes in, while ideally we would study these interaction with neutrinos, but the absence of monoenergetic neutrino sources, along with their small cross sections makes us consider other options. While on the surface it may seem different, electrons scatter off of nuclei in a similar manner, and further, nuclear effects are identical. Nuclear effects mainly come in two flavours, initial and final state effects.

Initial state nuclear effects describe how the state of the nucleus before the collision affects our measurements. An example that is seen in the results of this report is that if

the incident lepton scatters a nucleon outside the nucleus and we want to use 4 momentum conservation for analysis, we need to account for the non-zero 4 momentum of the original nucleon, and possibly also of the nucleus, neither of which are simple to model.

However, less predictable and likely more problematic are Final State Interactions (FSI), these can occur when the first (primary) lepton interaction creates or scatters other hadrons, which happens nearly always. These hadrons then start within the nucleus and can interact with it before escaping it. This is a significant effect, for $\sim$ 1GeV neutrinos impacting an iron target, about 30% of the created hadrons undergo FSI[16]. FSI can not only change the particle 4 momentum but also result in particle creation or absorption, completely changing the composition of the particles we detect. See [16, 17] for more detail.

2 Neutrino(Electron)-Nucleus Interactions

Firstly, throughout the report antineutrinos are largely not mentioned, their interaction do have some specifics to them, however are mostly directly analogous to the described neutrino processes. As the interactions are not yet fully, fundamentally understood, we to a large degree resort to classifications which allows us to make prediction under certain conditions. Both neutrino and electron nucleus scattering can be described by

$$l + A \rightarrow l' + a + b + c... \tag{3}$$

where an incoming lepton l scatters off of a nucleus A resulting in a lepton l' and hadron particles $a, b, c....$ When considering realistic experiments we always know l and A but might only be able to detect the outgoing lepton l' and some or none of the outgoing hadrons. To differentiate these cases we consider separately *inclusive* cross sections where only l' is detected (so any cross sections are essentially a sum over all possible outgoing hadrons). *Semi-inclusive* cross sections where l' and some of the hadrons are detected and *exclusive* cross sections where we know all of the resulting particles [18].

As neutrinos only interact via the weak force, all neutrino-nucleus interactions take place via either the Z^0 boson, in which case the final lepton is the same neutrino. These are called *Neutral Current* (NC) events and are generally difficult to measure as the outgoing lepton is undetected and we have to rely on reconstructing the event solely from the hadrons [19]. Or it can interact through the $W^+$and W^- bosons (*Charged Current* or CC interactions) in which case a charged lepton is produced and detected, often being the most important particle for event reconstruction.

This is contrasted to electrons which will dominantly interact with the nucleus through photons (so preserving the electron). Nevertheless within Quantum Field Theory (QFT) the electron EM and neutrino weak force interactions are modeled similarly and so theories for one can be tested on the other, see section 2.3 for more.

2.1 Particle and event properties

This is also a good place to introduce some of our notation and event properties. As these are high energy particles, we have to treat them relativistically, as such the key property of a particle is its 4 momentum p^μ, or equivalently energy E and relativistic 3 momentum

p. For our coordinate systems we choose the incident particle beam direction to be along the Cartesian e_z and we often use spherical polars with respect to this axis and such that $\theta = 0$ corresponds to e_z (often $\cos\theta$ is used instead of θ). The specific orientation of e_x and e_y isn't very important and so is mostly glossed over. In addition we use natural units in which $\hbar = c = 1$ and in the report we write 4 vectors such that the SR[2] metric $\eta_{\mu\nu}$ is diag$(1, -1, -1, -1)$ (though notably GENIE, ROOT, see section 2.3, and so our data analysis uses a convention where it is diag$(-1, -1, -1, 1)$). For example this means an incident particle of mass m and energy E would have 4 momentum

$$q_l^\mu \leftrightarrow \begin{pmatrix} E \\ \sqrt{E^2 - m^2} \\ 0 \\ 0 \end{pmatrix} \tag{4}$$

In the events we consider, we have an incident lepton with 4 momentum q_l^μ impacting the nucleus and let p_l^μ be the outgoing leptons 4 momentum. A very common scattering property within particle physics is the 4 momentum transfer q^2, here it is the 4 momentum change of the incident particle squared, so $(p_l^\mu - q_l^\mu)^2$, though within neutrino interactions typically $Q^2 = -q^2$ is used instead. Next, there is W, the invariant mass of all the produced hadrons, with regard to eq. (3), one of $a, b, c \ldots$ will be the remaining nucleus and $W^2 = r_\mu r^\mu$ where r^μ is the total 4 momentum of all the other hadrons. There are other commonly used event properties, notably the Bjorken scaling variables x, y, however they are not of interest in this report and so not covered.

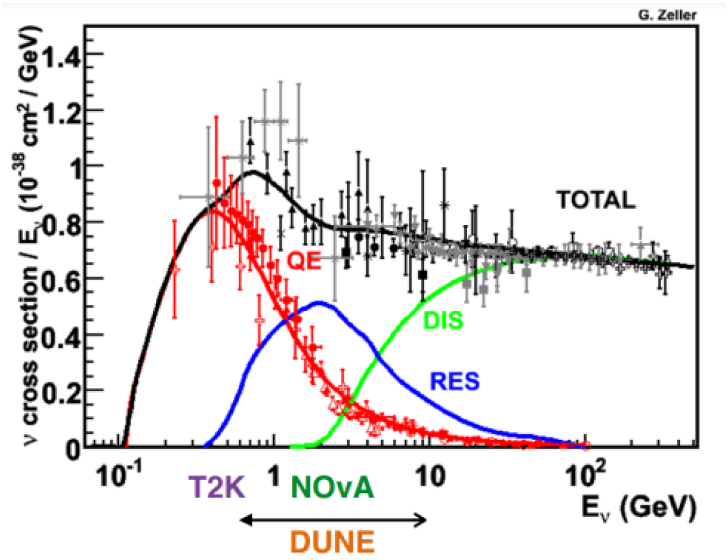

Figure 3: The differential cross section of neutrino-nucleus interactions shown for different interaction mechanisms and their sum. Near the x axis the approximate regions of interests for the T2K, NOvA and DUNE experiments is shown. Figure originally from [20].

[2]Special Relativity

2.2 Interaction types

Finally to come back to the interaction types mentioned at the start of section 2, some of the main types relevant for oscillation experiments are Quasi-Elastic (QE), Resonant (RES) and Deep Inelastic Scattering (DIS), see fig. 3. In this order these dominate at increasing energies and correspond with how far inside the nucleus the neutrino penetrated. Importantly, these classifications also carry over to electron scattering very well, in fact they are referred to within neutrino physics under the same names, even though QE electron scattering is closer to fully elastic scattering.

2.2.1 Quasi-Elastic (QE) scattering

In elastic scattering the structure of colliding objects isn't altered. Fully elastic neutrino scattering can then only happen within NC interactions. However, there is a very similar CC interaction where the neutrino interacts with a single neutron through an W boson, changing it into a proton, but otherwise conserving it's structure. This is shown in fig. 4, in many ways they are the simplest interaction as they don't require as much information about that nucleus theoretically and experimentally they have a very clear signature of one electron and one proton with FSI not playing a major role. Notably there are also equivalent NC QE processes where either nucleon type can be scattered outside the nucleus by an exchanged Z boson.

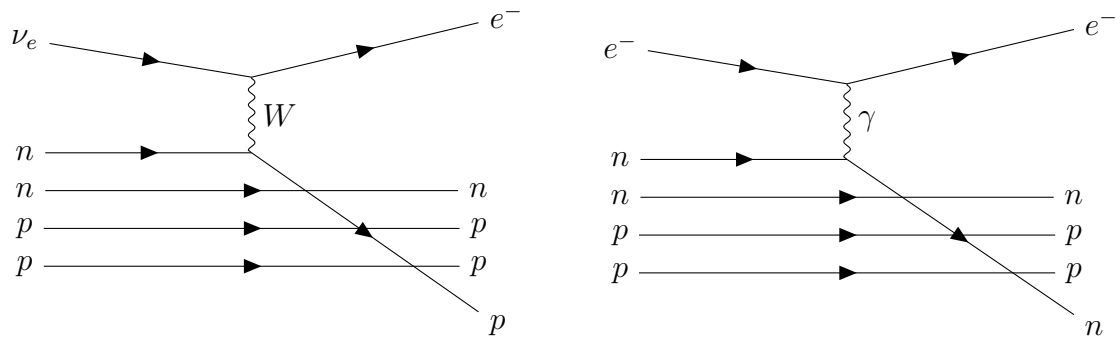

(a) One of the neutrons is converted to a proton and scattered outside the nucleus (making the nucleus a Helium 3).

(b) Here the electron only scatters one of the neutrons (or protons) out of the nucleus but it remains the same type.

Figure 4: A Feynman diagrams of typical QE interactions of an electron neutrino and an electron with a Helium 4 nucleus. (The W boson can be positive of negative depending on the time ordering.)

Of the neutrino interactions, QE are the best theoretically understood, the simplest models rely on a combination of two independent parts: calculations of neutrino-nucleon interactions within the impulse-approximation and modelling of the nucleons within the nuclei. A recent review [21] has compared the theoretical result with observations from the MiniBooNE and NOMAD. While the models capture many important features, there are also significant discrepancies which point to the interaction being more complicated than thought and also points out that many studies consider different levels of inclusiveness leading to difficulties in comparisons.

As they are not a focus of this work, we don't go further into detail, however it is worth saying that QE interactions are also a great example of the similarities of neutrino and electron scattering. Theoretically, QE neutrino scattering is very similar to elastic electron scattering off of nucleons in nuclei (also referred to as QE) and as electrons have been studied earlier it has served as inspiration for the neutrino QE scattering theories. Within e4ν the same data this report will be working with has been inspected for testing incident electron energy reconstruction for QE scattering in [22].

2.2.2 Resonant scattering (RES) with focus on Δ and pion production

Resonant interactions are dominant for neutrinos at energies near 1-2 GeV, they are the next logical step, the neutrino still only interacts with one nucleon, however this time that nucleon changes into an excited baryon state which promptly decays. There are a couple possible such excited states, called *resonances*, including various N and Δ particles with spins $\frac{1}{2}, \frac{3}{2}$ or possibly more [23]. Here we focus on Δ_{1232} resonances (with masses near 1232 MeV and spin $\frac{3}{2}$, throughout the report $\Delta \sim \Delta_{1232}$) as they are are some of the most dominant and suitable to study as they decay into pion and nucleon pairs with a branching fraction of 99.4% [24]. Other processes are largely similar to these.

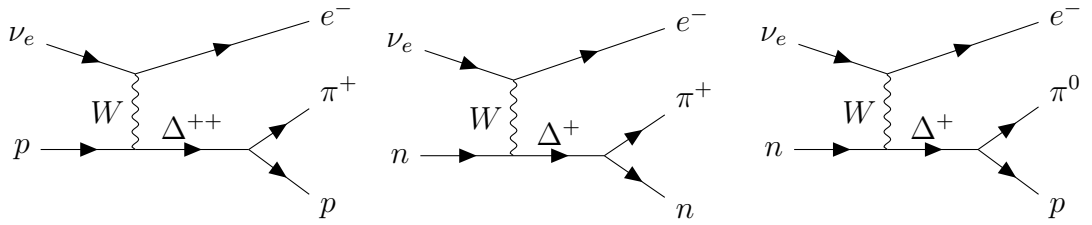

(a) $\pi^+ pe^-$ final state (b) $\pi^+ ne^-$ final state (c) $\pi^0 pe^-$ final state

Figure 5: All possible CC, Δ RES electron neutrino scattering processes summarized, only showing the relevant nucleon, the rest form the remaining nucleus. The processes are identical for ν_μ and μ_τ except with the other leptons replacing the final state electron.

The CC Δ RES processes for neutrino scattering are shown in fig. 5, and NC processes are analogous and summarized as

$$\nu + p \to \nu + \pi^+ + n \qquad \nu + n \to \nu + \pi^- + p \tag{5}$$

$$\nu + p \to \nu + \pi^0 + p \qquad \nu + n \to \nu + \pi^0 + n \tag{6}$$

and finally, the equivalent electron scattering processes are shown in fig. 6.

RES interactions are often studied as they are in many ways the next step in complexity after QE events and one of their distinctive features is pion production. This is important as pions can be detected by scattering experiments, though while charged pions have a mean lifetime of $\sim 10^{-8}$s, enough to reach a detector. π^0 have lifetimes of $\sim 10^{-17}$s [24] and decay into two photons before detection. They can then be reconstructed from photon measurements, however that adds complexity and so in this report we only look at charged pion events.

Other than RES interactions, pions can also be produced by coherent pion production where the neutrino/electron scatters off of the whole nucleus [25, 26] however at higher

energies these are less prominent compared to the other processes. Further pions can also be produced in FSI by any interaction type or in DIS interactions before FSI, however both of these typically create multiple particles and so are difficult to work with. For these reasons in our analysis we try to restrict the amount of these events in our sample, so that we can focus on simple pion production where the kinematics can be understood.

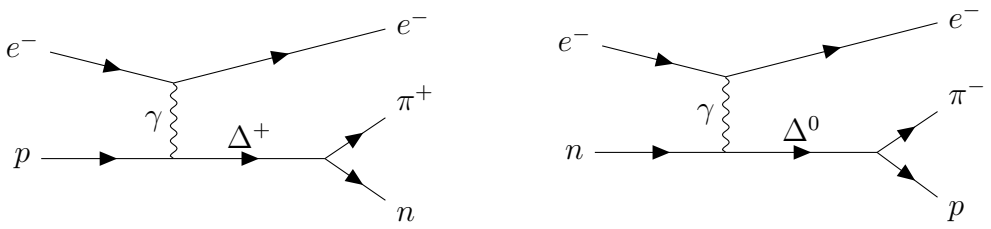

(a) π^+ne^- final state

(b) π^-pe^- final state

(c) π^0pe^- final state

(d) π^0ne^- final state

Figure 6: Δ RES electron scattering processes, (b) and (a) are the most important for this project as our data includes detected charged pions and protons.

2.2.3 Deep Inelastic scattering (DIS)

Finally at high energies ($>$ 3GeV) DIS events start to dominate, in these the neutrino scatters off of a quark within a nucleon (valence or sea quark). This typically results in a jet of multiple hadrons (can be pions, Kaons, strange sigma baryons... in the final state) and so W values are larger than in QE or RES, often over 2 GeV is mentioned[27]. They can take place through both NC and CC channels and there is again a connection to electron scattering, the models are similar and electron DIS scattering is one of the key probes of nuclear structure[28].

2.3 The GENIE event generator [29]

Due to the amount expertise required to understand either the theory or the experimental aspects of neutrino interactions, it becomes difficult to package theories in a way that they can be easily understood and tested by experiments. Partly due to this the Neutrino Scattering Theory-Experiment Collaboration (NuSTEC [30]) has been started recently. As a result, Monte Carlo (MC) neutrino event generators are used to package theoretical models in a way that predictions can be made. GENIE is the most widely adopted such MC generator, first released for use in 2007 it aims to be a canonical generator accurately reflecting the state-of-art theories for a wide range of energies and targets. It is a large codebase of modern C++ code using the popular ROOT framework[31] and is particularly

well tuned to a tested on the few GeV energy neutrinos that are of interest to oscillation experiments.

As is described in [29, 32], there are three main steps of models in GENIE. Nuclear physics models describe the nuclei and their composition as experienced by the incoming neutrino (initial state effects). GENIE uses a Relativistic Fermi Gas (RFG) model for this step which is particularly successful at lower energies. Then cross sections are calculated for various scattering types using their cross-section models and one is randomly chosen according to these. These types include the ones mentioned in section 2.2, but they are both further divided and other interactions are considered, including NC scattering and neutrino-electron scattering. Hadronization models then finalize the primary interaction by predicting which hadrons are produced, for these GENIE uses the AGKY model from the MINOS experiment [33].

However there are various ways to tune this models according to experimental or theoretical data. The two main tuning setups used by e4ν are the G2018 (somewhat more empirical separating the different interactions earlier) and GSuSAv2, which we use here, this uses a super-scaling lepton scattering model[34].

Importantly, GENIE also has an electron scattering mode (e-GENIE) that has been revised in 2021 by the e4ν collaboration [35]. Within QFT the neutrino weak force interactions have vector and axial-vector components and the electron EM interaction only has a vector component. The theory is beyond the scope of this report, but the key is that the vector component code logic and structure can be used for generating electron-nucleus interaction events (provided adapted tunings). We can then compare e-GENIE data to electron scattering experiments to test the same underlying GENIE models as for neutrino scattering. This is at the core of the e4ν project.

3 The e4ν CLAS6 Data and Writing the Analysis Code

The data used by the e4ν analysis comes from the e2a experiment measuring electron scattering at electron energies of 1.16, 2.26 and 4.45 GeV on targets of He, C and Fe nuclei. The measurements took place in Thomas Jefferson National Accelerator Facility (JLab) using the CEBAF Large Acceptance Spectrometer (CLAS6) [36] in 1999, the data has been used in many published works including [22, 37]. In addition, recently CLAS has undergone an upgrade (CLAS6 to CLAS12) [38] allowing experiments at electron energies up to 12 GeV and generally improved capabilities. The e4ν collaboration has a CLAS12 experiment under development, with new data starting at electron energies of $\sim$ 6GeV expected to be ready soon. Along with measured data events we also have collections of GENIE generated events for the same energies and targets (the $\sim$ 2GeV neutrino energy C target has 1 million measured and 175 million GENIE generated events).

3.1 CLAS6

The CLAS6 detector is largely built around a set of six toroidal magnets distributed along the azimuthal angle ϕ. These curve the trajectories of charged particles in their ϕ plane and allow for charged particle momentum measurements in drift chambers. They

also give rise to six distinct sectors visible in fig. 7 and deadspace between them from particles hitting the magnets.

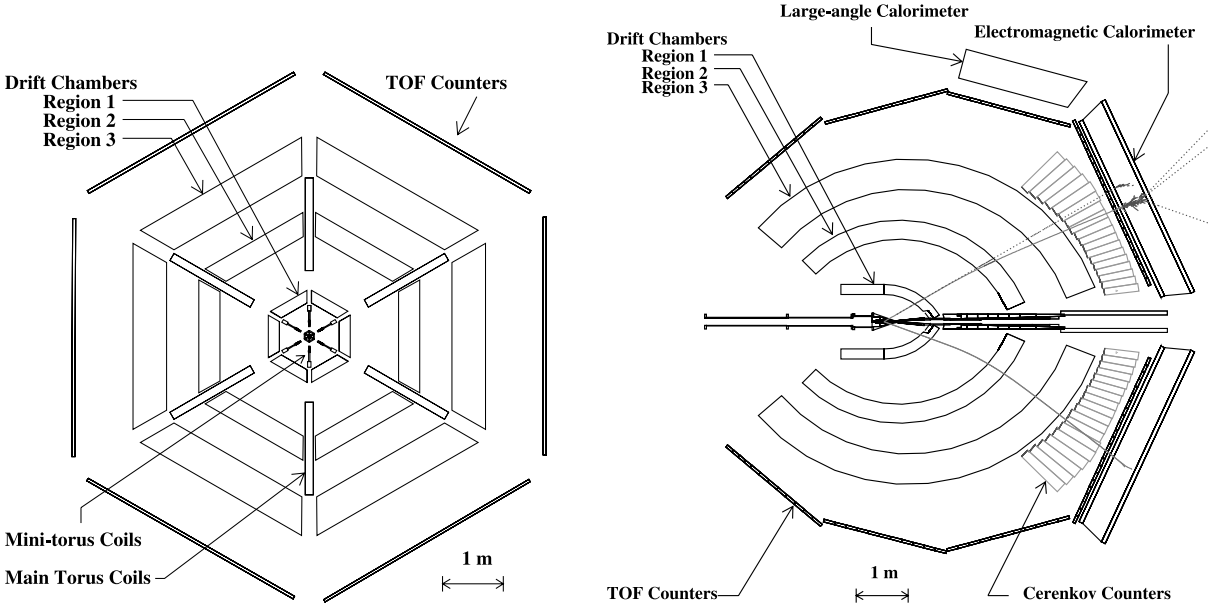

(a) CLAS6 as seen along the beam axis.

(b) Side view cross section through the detector.

Figure 7: Diagrams of the CLAS6 detector from [36], see for more detail. Most important for us are the EM calorimeter spanning $\theta < 50°$ which detects the scattered electrons and photons. Cherenkov counters near the axis are needed for distinguishing electrons and negative pions and the time-of-flight (TOF) detectors help distinguish protons and positive pions.

Our data, from e2a, has measurement of electrons, protons, charged pions and photons (so our cross sections are inclusive over all the other particles), each event having a list of 4 momentum measurements for each detected particle. In order to compare measured and MC data it is first necessary to take into account the detector limitations of only detecting particles in certain regions and with finite probabilities. This can be done by thoroughly considering all the possible ways the event measurements could have taken place and correcting for each in order to produce a measurement of the true physics. This is however very complicated and error prone and if one only needs to test a certain aspect or a model it is much easier to degrade MC data according to the detector defects for comparison. This is what we do in this report though we only look at MC data.

3.2 Fiducials and acceptance maps

We do this in two ways, first we use *fiducial* cuts. These are a set of conditions for each particle type to match, they depend on the particles momentum and direction and are boolean, either pass or fail. They reflect the harder boundaries in which we would expect out detector to work, we apply these to both measured and MC data and they define what events we consider our signal. These we inherited from previous e4ν and e2a analysis as a collection of C++ files, projections for some are shown in fig. 8 (the gaps reflects detector defects on the day of the run) and see [37] appendix C for more detail.

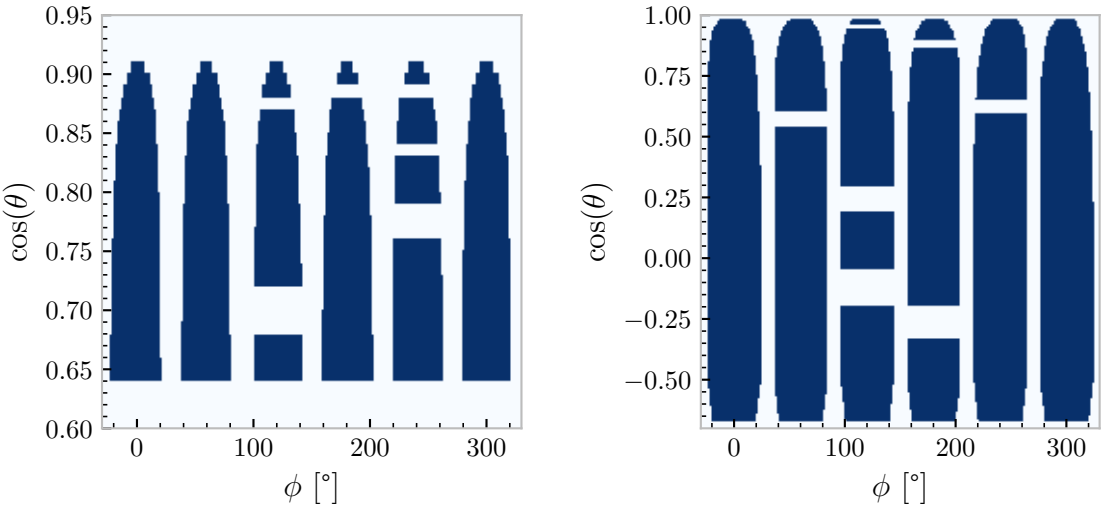

(a) e^- at a momentum of 1GeV (b) π^+ at a momentum of 0.7GeV

Figure 8: Showing the directional dependence of our fiducial cuts for data with beam energy 2.26GeV. The fiducials for electrons and positive pions at fixed 3 momentum magnitudes are shown, dark blue means the particle passes, grey that it is cut. ϕ angle is shown in the -30 to 330° range, this is in order not to cut through the accepted segment.

Then for true MC to experiment comparisons we use *acceptance* maps. These have been compiled by e2a as well, this time as 3D histogram ROOT files with $|\mathbf{p}|, \cos(\theta)$ and ϕ as axes. They are separate for each detected particle type and assign a probability of detection based on particle 3 momenta, see fig. 9.

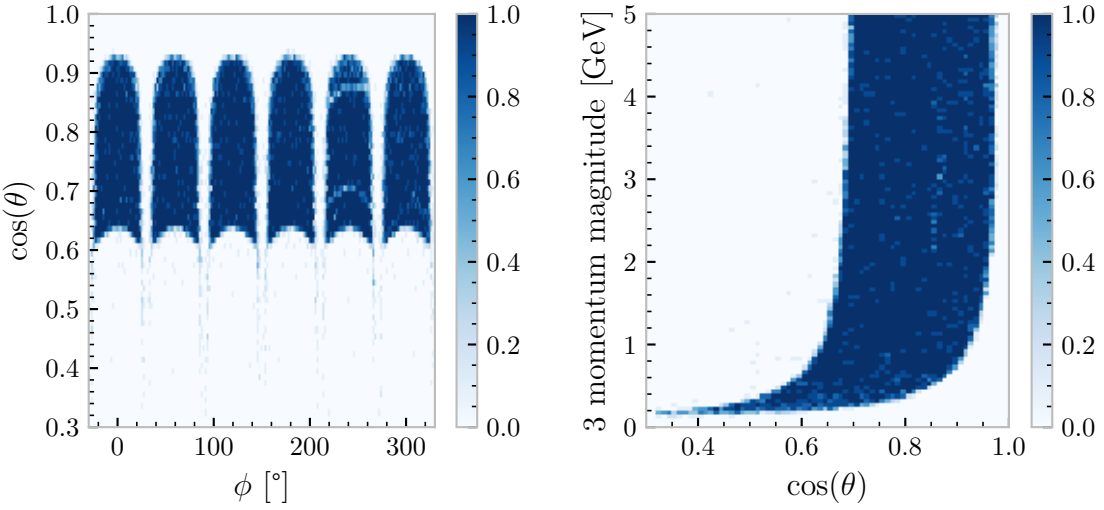

(a) Fixed $|\mathbf{p}| = 1$GeV (b) Fixed $\phi = 0$

Figure 9: Electron acceptance map projections for the 2.26GeV beam energy and C target dataset. The z, colormapped axis is the probability of an electron in the region being accepted.

3.3 Analysis details and the new framework

These datasets are each in a ROOT file in a GENIE format called `gst`, this is a list-like object (ROOT `TTree`) of events with their properties. Some of the more notable fields are the outgoing electron 4 momentum, information about all the particles after the neutrino-nucleus interaction (referred to as primary or initial state) as well as the same information about post FSI particles (final state). Some of these properties, especially the ones that never could be measured (and so empty in measured data), are referred to as the "truth" as they reflect the true physics. There are also flags to separate QE, different RES and DIS events and information on what FSI has taken place, this is best described in the GENIE manual[32] though it is somewhat outdated.

As there are ~ 100 different properties per event and up to hundreds of millions of events, a moderately sophisticated analysis code is needed. The main e4ν code is available on github [39] as developed by Afrodite Papadopoulou for her thesis[40], however it has since been used by various scientists each adding their own functionality. As a result there are various versions kept by people of a large and very difficult to understand code, most the logic of the analysis being in a single 4000 line file. A main goal of this project was to redevelop this code in order to lower the entry barrier for others (including future students), make it easier to spot analysis flaws and reduce boilerplate code.

The newly developed code is also available on github [41], it uses C++17 features and ROOT 6.12 as available on the GENIE machine at Fermilab used by us. It heavily uses classes and the features are best described by describing the code. The main class `GenieAnalysis` will expect an input file with a `gst` dataset, has two virtual methods to be overriden `double passesCuts()` and `void useEntry(double weight)` and one method that is expected to be used `void runAnalysis(int number_of_entries)`[3]. The last of which will start an analysis, it will go through the first `number_of_entries` events from the input file and for each `passesCuts` will be ran, its return value being used as the weight, so if it is zero that event is not used at all. If non-zero, `useEntry(weight)` is called with that weight, this method does nothing in this class, it is expected to be overriden by inheriting classes to for example count the events, or write some properties to a histogram.

The likely most useful part of the code is the `GAAutoHistograms` class, this builds on top of `GenieAnalysis` and provides automatic ROOT histogram generation for event "properties", say W or outgoing electron energy. A concept of event "type" is also defined in the code, one might be QE events or another may be all events, the property histograms are then generated for each type independently. The class has an easily extensible (couple lines of code) list of "known" properties and types and then the user only needs to provide a list of histograms to generate. Specifically there are two types of histograms that can be created, 1D histograms for each property, and also 2D histograms showing the correlation of some 2 chosen properties.

Some more information on the code is in appendix B and on the github repository[41].

[3] I am somewhat loose with the code for the sake of brevity, for example replacing the ROOT types with the normal C++ ones.

4 Nuclear Transparency of 1 Pion 1 Nucleon Events

Finally, once all the preliminary coding has been completed, we conduct a basic nuclear transparency study on the data. Nuclear transparency is a very wide term describing how significant nuclear effects are under certain conditions. Given its nature nuclear transparency is often studied either theoretically or from MC data as we cannot measure any particle properties before FSI.

Here we look at events with 1 charged pion 1 nucleon from a GENIE generated dataset and inspect how well we can reconstruct the pion momentum from the electron and nucleon momenta. We use the datasets mentioned before, they are described in more detail in [40], and specifically we only look at the data with beam energy of 2.26GeV and mainly carbon target. Importantly, GENIE was tuned to the SuSAv2 configuration using the INTRANUKE hN model for FSI (called "intranuclear transport modelling" in the GENIE documentation[32]). GENIE has two models for FSI, hA and hN, the main difference being the hA modelling a hadrons path out of the nucleus as a whole, either it scatters once or not at all. hN performs a full IntraNuclear Cascade (INC), each hadron can rescatter multiple times including hadrons produced from a previous rescattering, of the two hN is the more accurate though slower model[32].

The pion reconstruction is done as for simple pion production of exactly 1 charged pion and 1 nucleon without any FSI, the main channels of this process we are looking for are the Δ resonances showed in fig. 6. We then further assume the struck nucleon to be at rest and the reconstruction goes as follows. Denoting the 4 momenta of the electron and nucleon before collision as q_e^μ and q_n^μ, both of which we know. Their sum must be equal to the sum of the 4 momenta of the outgoing electron, pion and nucleon, denoted respectively as p_e^μ, p_π^μ and p_n^μ.

$$q_e^\mu \leftrightarrow \begin{pmatrix} E_b \\ \sqrt{E_b^2 - m_e^2} \\ 0 \\ 0 \end{pmatrix} \qquad q_n^\mu \sim \begin{pmatrix} m_n \\ 0 \\ 0 \\ 0 \end{pmatrix} \tag{7}$$

$$\begin{aligned} q_i^\mu + q_n^\mu = p_e^\mu + p_\pi^\mu + p_n^\mu \implies \\ p_\pi^\mu = q_i^\mu + q_n^\mu - p_e^\mu - p_n^\mu \end{aligned} \tag{8}$$

Of course for the data this will rarely work perfectly, we expect 3 main sources of errors – the original nucleon having non-zero momentum, other pion production processes producing other undetected particles, mainly other RES and DIS, (photons, other mesons...) and finally FSI. However they all have different signatures and so we can largely separate them, first we however need to define our signal.

We have conducted many runs with different parameters, they can be summarized by three options, which event set we use, which combination of charged pion and nucleon we are looking for and if we do a cut on W. The event sets and W cut are described below and the pion/nucleon combination is fairly self-explanatory. Data for all 4 of these combinations was collected though as they are largely the same we focus on $1\pi^-1p$ events as this is the only combination produced by Δ resonances that we have fiducials and acceptances for both of the particles.

4.1 The event sets

The 4 different event sets are the Primary State (PS), Final State with no Rescattering (FSR), any Final State (FS) and Detector Like (DL) runs. For all of them we use the CLAS6 fiducial cuts, for PS, FSR and FS the first part is the same, we check if the electron 3 momentum passes the fiducial cuts and the event is only used if it does.

Primary State (PS) is the closest to the "truth"/physics we get here. After checking the electron fiducials, particle data from the GENIE reported primary state (GENIE label, means before FSI) is used. The code then goes through all the produced hadrons and only charged pions and protons that pass their fiducials are considered, along with all neutrons (we don't have fiducials for them as they weren't detected in the e2a CLAS6 data). Only if there are exactly 1 charged pion and 1 nucleon of the required types and 0 of the others, is the event used. Notably there is another way the fiducials could be applied, we could only consider event where all charged pions and protons pass their fiducials and only then check their numbers. This method was also tried and resulted in near identical results and so it suggests the decision isn't a major one.

Final State with no Rescattering (FSR) should in theory and we observe it to be almost the same as PS. GENIE also reports for each particle in the primary state a `resc` code specifying if and in what way did that primary state particle rescatter in FSI. In FSR the final state (means post FSI) particle properties and 3 momenta are used, however only events where all the `resc` codes indicated no rescattering. The final state particles are then processed in the same way as in PS, only particles passing fiducials are considered and the counts of charged pions and nucleons must exactly match.

Final State (FS) means we use final state particles and their properties just as in FSR, but do no checking of `resc`. This should result in increased noise and for example getting pion plus nucleon events even from QE scattering as they can be produced in FSI.

Detector Like (DL) This is to get some insight into what level of precision we might expect from detector data. This event set introduces an additional element of Monte Carlo methods, starting with the electron, if it passes the fiducial cuts its acceptance is calculated. Then according to the acceptance likelihood it is randomly either accepted or rejected, if accepted the 3 momentum magnitude will be smeared in the same way that previous e4ν work has used [40]. This is done by drawing a number from a Gaussian distribution with mean of the original distribution and σ of 0.005 times the original magnitude.

Then for the hadron particles, we use particle from the final state that pass their fiducial cuts. Then as in our case neutrons aren't detected they are taken at this stage, however for charged pions and protons their acceptances are calculated and are either accepted or rejected randomly according to them in the same way as electron. Their 3 momenta are then also smeared in the same way this time using 0.007 for charged pions and 0.01 for protons as the scaling factor for σ.

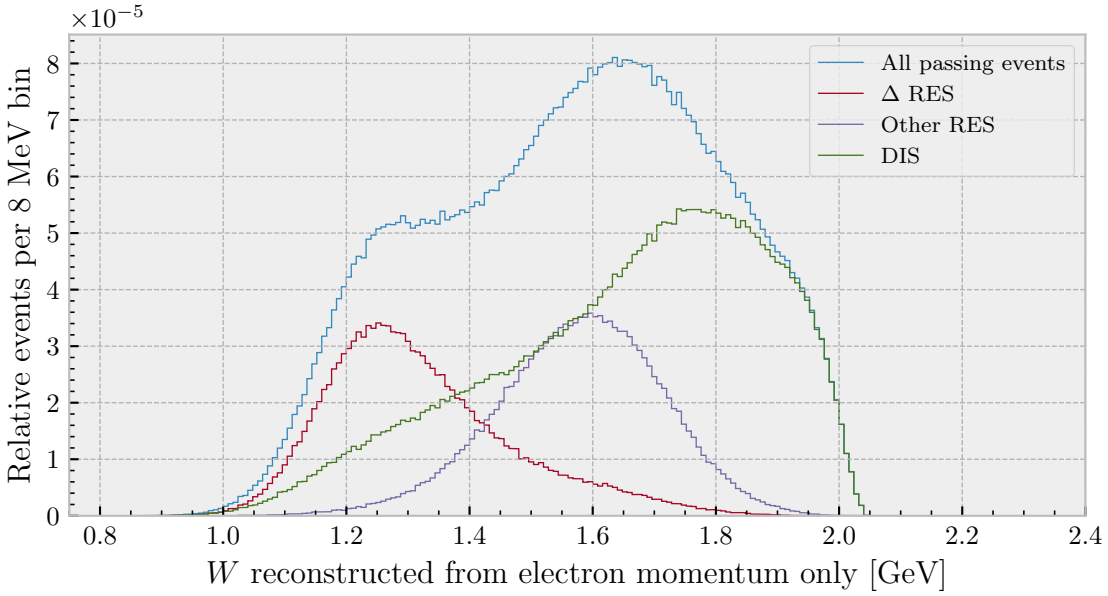

Figure 10: W distribution for the PS, $1\pi^{-}1p$ event set without the W cut, there are no QE events as they never produce pions before FSI. The relative number of events is the number of passing events in the bin divided by all the events in the dataset (∼175 million) before any fiducials. Carbon target and 2.26GeV beam energy.

4.2 The W cut

This is an extra cut to try to separate the Δ resonances using only properties known to experiments. Also note that again assuming the struck nucleon being at rest[4] we can calculate $W^2 = r_\mu r^\mu = (q_e^\mu + q_n^\mu - p_e^\mu)^2$ and so reconstruct W solely from the electron 4 momentum. Figure 10 shows a histogram of the electron reconstructed W values for one of the runs split by different interaction types, similar plots are often produced by studies. As we have selected only pre FSI pion production events there are no QE events, otherwise they would form a narrow peak near 1GeV. The peak of the non-Δ RES corresponds to the N masses and DIS events typically come in behind them and with a sharp drop off near 2GeV as the incident electrons have energy 2.26GeV. If we then only consider events in some range of W values we can change the relative dominance of the interaction types.

This process can of course be done with any event property, we choose W as previous work by Lucas Taling in his MSc thesis[42] has shown that it is the ideal choice for separating Δ resonances. We then choose the optimal cut value by considering purity, the number of passing Δ events over all passing events, and efficiency, the number of passing Δ events over all Δ events. Figure 11 shows a sample plot of these quantities along with their product which we choose as our metric for choosing the cut. Only one such plot is shown, but all the others are very similar and give values of 1.4 ± 0.02GeV for the optimal cut thus we use 1.4GeV.

[4]This method for W reconstruction is often used (GENIE calculates such a value) though even if it was incorrect in terms of being equal to the hadronic invariant mass, its use as a cut still holds.

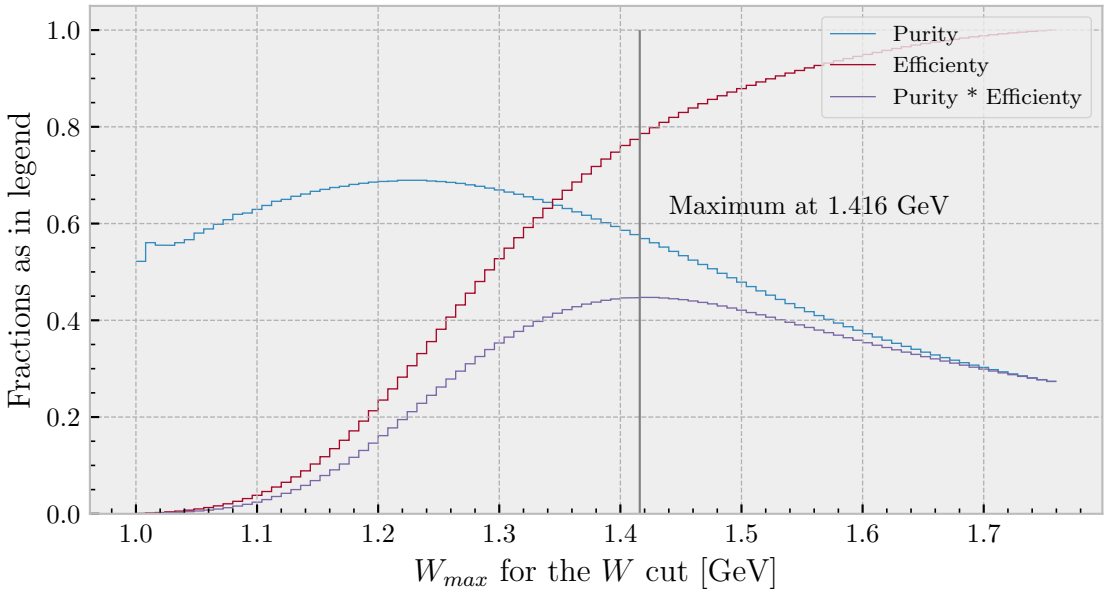

Figure 11: The performance of the W cut for the PS, $1\pi^{-}1p$ no W cut event set, purity and efficiency as defined above in text. Numbers are calculated directly from the W histogram, hence the steps. Carbon target and 2.26GeV beam energy.

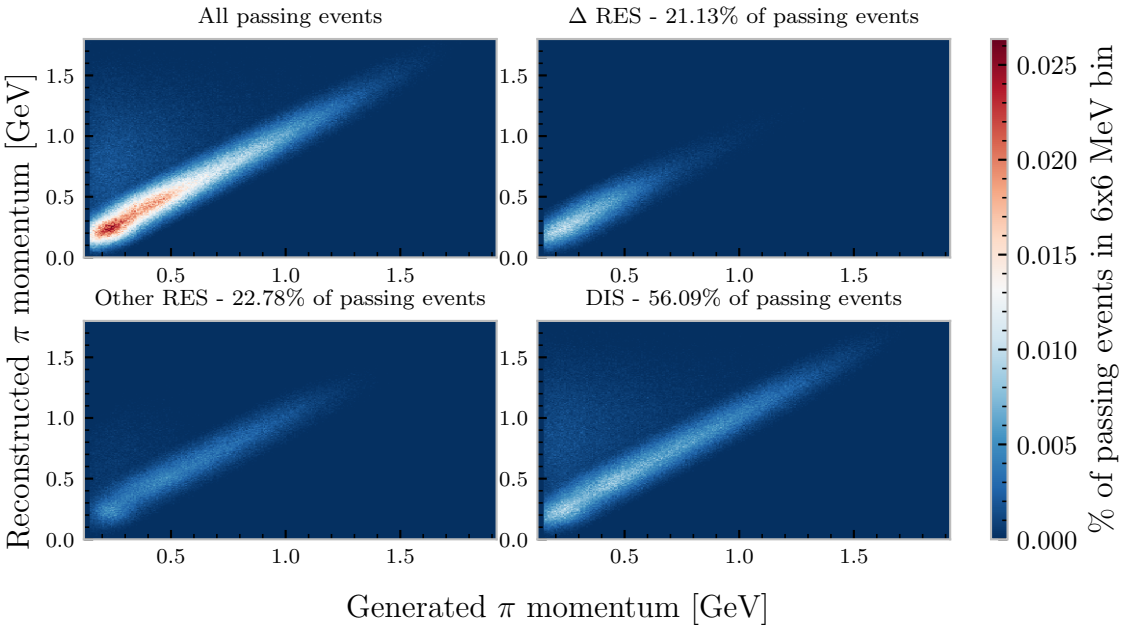

Figure 12: Correlation of actual and reconstructed pion momentum magnitude for the $1\pi^{-}1p$, PS, no W cut data. The Δ events have a near constant width due to the original nucleon non-zero momentum and no off diagonal events. Other RES events and DIS both have the same width and also off diagonal events as they will more commonly produce other unaccounted for particles including photons and mesons. Carbon target and 2.26GeV beam energy.

4.3 Primary state results

The first useful quantities come from the PS run where we can also check the `resc` codes of the pion and nucleon and see how often they do rescatter in FSI. See table 1 for these results, these are plausible within other literature numbers, [16] quotes a 20% chance of a pion being absorbed in a carbon nucleus. In our data we see 20% and 21% for $1\pi^{-}1p$ and $1\pi^{+}1n$ respectively, other rescattering mechanisms accounting for the rest.

	$1\pi^{-}1p$	$1\pi^{+}1n$
% of events with no π rescatter	63.9	61.8
% of events with no nucleon rescatter	77.7	74.3

Table 1: FSI rescattering rates for PS event sets without W cut, of carbon target at beam energy 2.26GeV.

For a qualitative look at the pion momentum reconstruction performance, 2D histograms of events with respect to actual and reconstructed pion momentum magnitude are the most useful. Figures 12 and 13 show these for the PS, $1\pi^{-}1p$ and $1\pi^{+}1n$ event sets. Also note that there is no separate diagram for QE events, for PS and FSR event sets there are none as pions are only created in FSI for QE events. Some QE events did appear for FS and DL event sets (due to FSI pion production) however at most 1% of the events (see table 2 in appendix A) and only constitute noise.

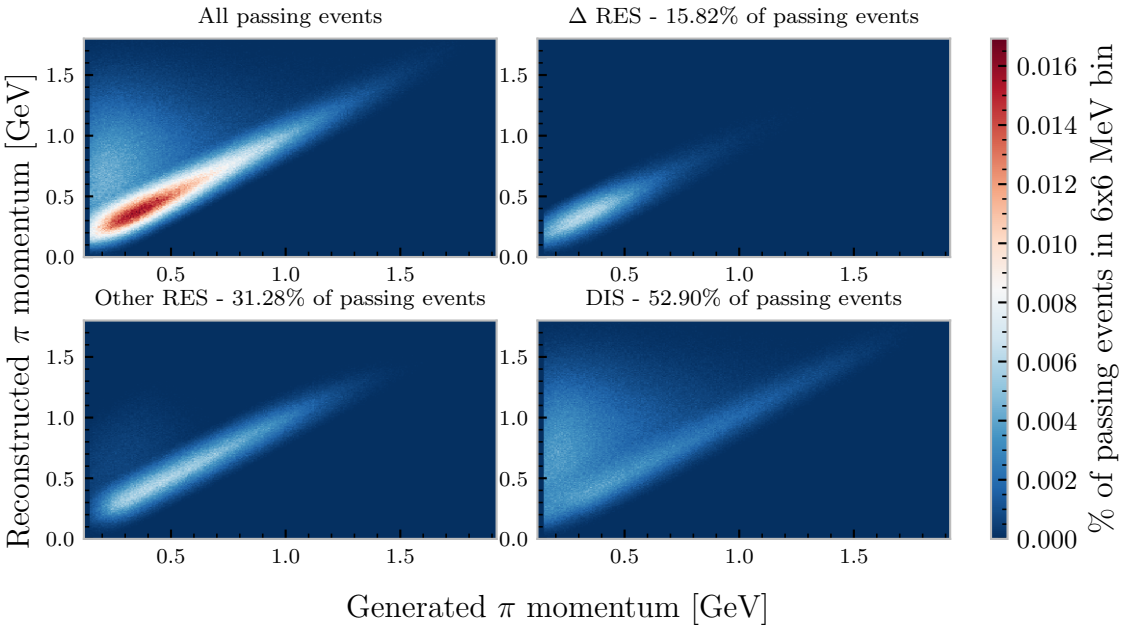

Figure 13: Correlation of actual and reconstructed pion momentum magnitude for the $1\pi^{-}1p$, PS, no W cut data. Same observations apply as to fig. 12 though are many more events here due to the lack of fiducials for n. Carbon target and 2.26GeV beam energy.

The main difference between figs. 12 and 13 is that the $1\pi^{+}1n$ has more events and less of the events are from Δ RES. This shows that the fiducials already significantly

help separating other RES and especially DIS events. The main result from both is that all Δ events are distributed along the diagonal, meaning the reconstruction works as it should with the width being due to the non-zero struck nucleon momentum[5], an initial state effect and showing this can act a probe of nuclear structure.

Finally, the FSR event set yields exactly the same event properties as PS except dropping events where any FSI rescattering occurred. As such the FSR plots add little value (and are shown in appendix A, fig. 17), the only notable difference being a significant drop in event counts near pion momentum $\sim$ 270MeV. This is an interesting result as it points to pions or nucleons experiencing an increase in FSI interactions near the area and the same gap is visible in FS and DL data.

4.4 Detector like and other results

Moving on to data more likely to reflect experiment, FS and DL show similar features and no differences between $1\pi^-1p$ and $1\pi^+1n$ other than those pointed out before, so I only focus on the DL, $1\pi^-1p$ event set. Without the W cut we get similar results as in fig. 12 but with added noise and the mentioned lack of events near pion momentum of 270MeV, notably however only 16% of the events are Δ RES and 64% are very noisy DIS events. The data with W cut applied is shown in fig. 14, with 54% of events now being Δ RES a significant improvement showing the cuts' performance.

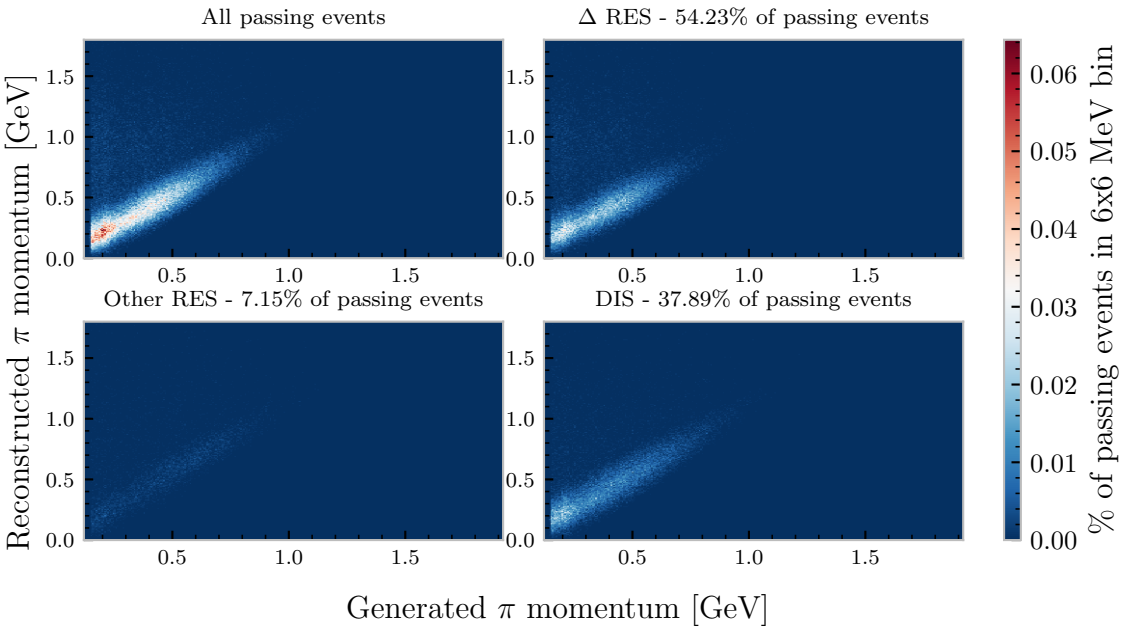

Figure 14: Correlation of actual and reconstructed pion momentum magnitude for the $1\pi^-1p$, DL, data with the W cut applied. The Δ events are noticeably affected by FSI. The W cut works very well on the other RES though further DIS event separation could be desirable. Carbon target and 2.26GeV beam energy.

Another parameter of note is the actual and reconstructed pions 3 momentum mag-

[5]The fact that visually the width seems to decrease is just an effect from there being less events at higher momenta.

nitude difference, call it $\Delta p = |\mathbf{p}_{\text{reco}}| - |\mathbf{p}_{\text{actual}}|$. While this may be viewed as misleading due to subtracting vector magnitudes instead of getting the magnitude of the vector difference, the two vectors are mostly in the same direction (the directional reconstruction performs well, shown in appendix A, fig. 19) and overall the number is a good qualitative metric.

This is shown in fig. 15, the width of the zero centered peak is $\sim$ 400MeV, this is mainly due to initial nucleon momentum and detector smearing. Also $\sim$ 12% of the events are in the right hand side tail ($\Delta p > 220$MeV) caused by unseen particles mainly from FSI (we also checked for correlation between Δp and the real pions momentum and there was none, further supporting the width coming from the original nucleon). These are fairly promising results in terms of using the reconstruction method on measured data within the same energy range and target. Though the effects of unseen particles particularly from FSI are significant and further efforts for isolating 1 π 1 nucleon events would be worth pursuing.

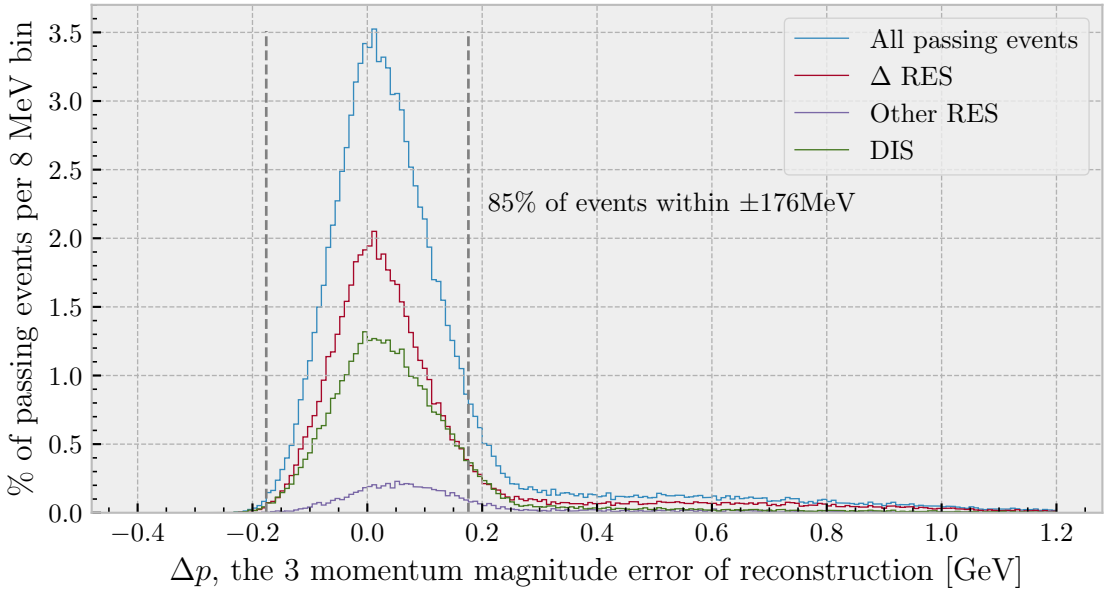

Figure 15: Reconstructed and actual pions momentum magnitude difference for the $1\pi^{-}1p$, DL data with the W cut applied. The width of the peak around 0 comes from the initial nucleon momentum and the tail to the right from events with additional unseen particles. These carry some of the momentum thus decrease actual pion momentum. Carbon target and 2.26GeV beam energy.

Finally, on a separate note if we use the actual pion momentum information we can using eq. (8) calculate essentially the GENIE modeled momentum of the original nucleon. This shows how electron experiments are used to probe nuclear structure and is a good sanity check, our data, shown in fig. 16, agrees quite well with data from [43].

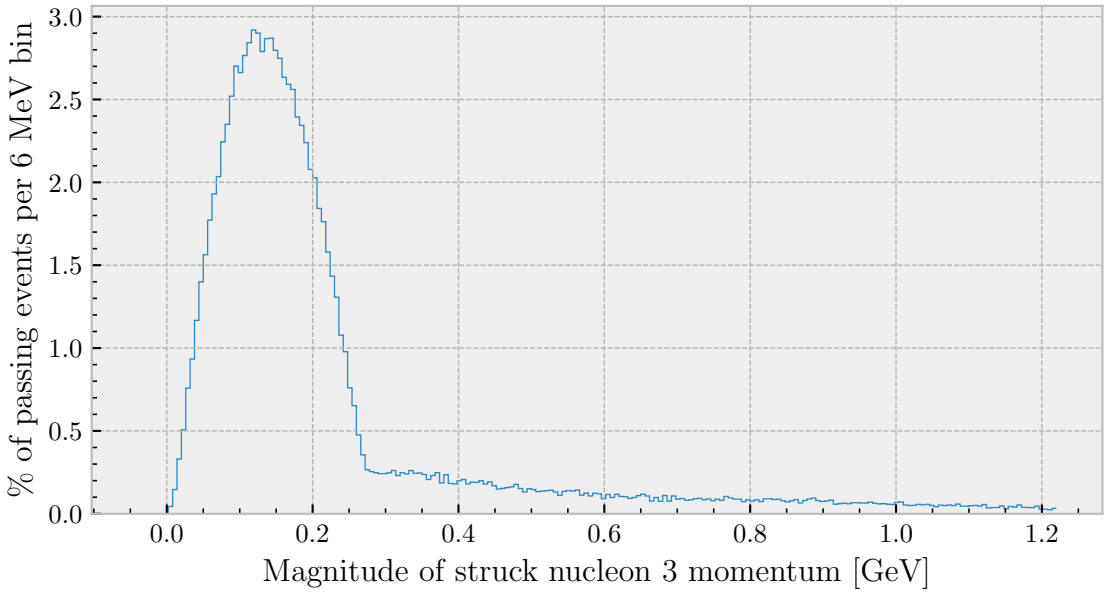

Figure 16: Momentum of the struck nucleon as reconstructed using actual pion momentum from the $1\pi^{-}1p$, DL data with the W cut. Carbon target and 2.26GeV beam energy.

5 Conclusion

As a part of this project a new data analysis framework for both measured and MC data (in `gst` format) has been developed. Hopefully significantly decreasing the entry barrier for future projects, the framework is easily adaptable (to say the new CLAS12 data) and provides a more modern object oriented interface.

The framework was then used for a nuclear transparency study of $1\pi 1$nucleon events on 2.26GeV electrons scattering off of carbon nuclei, using the GENIE MC generated data from the e4ν CLAS6 dataset. For that purpose we used a simple 4 momentum conservation method to reconstruct the pion momentum from the electron and nucleon kinematics. This targets simple pion production events not producing any other particles, we in particular focused on the Δ resonant $1\pi^{-}1p$ production events. We also used the CLAS6 fiducial maps and a W cut at 1.4GeV in order to maximize the number of such events in our data.

The reconstruction shows promising results with 85% of the events being reconstructed to within $\pm$180MeV for $1\pi^{-}1p$ events with the W cut, where we accounted for detector uncertainties using acceptance maps. There are two main error contributions, nuclear initial state effects are responsible for the correctly identified states having a mean error of $\sim$ 150MeV in the momentum reconstruction. Likely more concerning are however the remaining $\sim$ 15% of misidentified events, mainly coming from FSI and DIS events, For these the reconstruction does not work and further event selection may be required in order use the reconstruction on experimental data.

References

[1]T. Potter, *5. Feynman Diagrams - Particle and Nuclear Physics*, https://www.hep.phy.cam.ac.uk/~chpotter/particleandnuclearphysics/Lecture_05_FeynmanDiagrams.pdf (visited on 02/22/2023).

[2]H. Burkhardt, J. Lowe, G. J. Stephenson, and T. Goldman, "The wavelength of neutrino and neutral kaon oscillations", Physics Letters B **566**, 137–141 (2003).

[3]K. Zuber, *Neutrino physics*, Third edition., Series in High Energy Physics, Cosmology & Gravitation (Taylor & Francis, Boca Raton, FL, 2020).

[4]A. de Gouvêa, B. Kayser, and R. N. Mohapatra, "Manifest CP violation from Majorana phases", Physical Review D **67**, 053004 (2003).

[5]R. B. Patterson, "The NOvA experiment: status and outlook", Nuclear Physics B - Proceedings Supplements, The XXV International Conference on Neutrino Physics and Astrophysics **235–236**, 151–157 (2013).

[6]K. Abe et al., "The T2K experiment", Nuclear Instruments and Methods in Physics Research Section A: Accelerators, Spectrometers, Detectors and Associated Equipment **659**, 106–135 (2011).

[7]A. Falcone, "Deep underground neutrino experiment: DUNE", Nuclear Instruments and Methods in Physics Research Section A: Accelerators, Spectrometers, Detectors and Associated Equipment **1041**, 167217 (2022).

[8]M. Yokoyama, *The Hyper-Kamiokande Experiment*, (Apr. 30, 2017) http://arxiv.org/abs/1705.00306 (visited on 03/30/2023), preprint.

[9]M. Mezzetto and F. Terranova, "Three-Flavor Oscillations with Accelerator Neutrino Beams", Universe **6**, 32 (2020).

[10]R. Acciarri et al., "Design and construction of the MicroBooNE detector", Journal of Instrumentation **12**, P02017 (2017).

[11]K. S. McFarland, "MINERA: a dedicated neutrino scattering experiment at NuMI", Nuclear Physics B - Proceedings Supplements, Proceedings of the 4th International Workshop on Neutrino-Nucleus Interactions in the Few-GeV Region **159**, 107–112 (2006).

[12]M. Sajjad Athar, A. Fatima, and S. K. Singh, "Neutrinos and their interactions with matter", Progress in Particle and Nuclear Physics **129**, 104019 (2023).

[13]I. B. Whittingham, "Scattering of low energy neutrinos and antineutrinos by atomic electrons", Physical Review D **105**, 013008 (2022).

[14]K. Abe et al., "Constraint on the matter–antimatter symmetry-violating phase in neutrino oscillations", Nature **580**, 339–344 (2020).

[15]NOvA Collaboration et al., "New constraints on oscillation parameters from ν_e appearance and ν_μ disappearance in the NOvA experiment", Physical Review D **98**, 032012 (2018).

[16]S. Dytman, "Final State Interactions in Neutrino-Nucleus Experiments", Acta Physica Polonica Series B **B40**, 2445–2460 (2009).

[17]T. Golan, C. Juszczak, and J. T. Sobczyk, "Effects of final-state interactions in neutrino-nucleus interactions", Physical Review C **86**, 015505 (2012).

[18]J. E. Amaro, M. B. Barbaro, J. A. Caballero, R. González-Jiménez, G. D. Megias, and I. R. Simo, "Electron- versus neutrino-nucleus scattering", Journal of Physics G: Nuclear and Particle Physics **47**, 124001 (2020).

[19]C. Giusti and M. V. Ivanov, "Neutral current neutrino-nucleus scattering: theory", Journal of Physics G: Nuclear and Particle Physics **47**, 024001 (2020).

[20]J. A. Formaggio and G. P. Zeller, "From eV to EeV: Neutrino cross sections across energy scales", Reviews of Modern Physics **84**, 1307–1341 (2012).

[21]H. Gallagher, G. Garvey, and G. Zeller, "Neutrino-Nucleus Interactions", Annual Review of Nuclear and Particle Science **61**, 355–378 (2011).

[22]M. Khachatryan et al., "Electron-beam energy reconstruction for neutrino oscillation measurements", Nature **599**, 565–570 (2021).

[23]T. Leitner, O. Buss, L. Alvarez-Ruso, and U. Mosel, "Electron- and neutrino-nucleus scattering from the quasielastic to the resonance region", Physical Review C **79**, 034601 (2009).

[24]Particle Data Group et al., "Review of Particle Physics", Progress of Theoretical and Experimental Physics **2022**, 083C01 (2022).

[25]H. Sogarwal and P. Shukla, "Coherent pion production in neutrino (anti-neutrino)-nucleus interaction", Nuclear Physics A **1027**, 122494 (2022).

[26]A. Higuera et al., "Measurement Coherent Production of $\pi^{\pm}$ in Neutrino and Anti-Neutrino Beams on Carbon from E_{ν} of 1.5 to 20 GeV", Physical Review Letters **113**, 261802 (2014).

[27]J. G. Morfín, J. Nieves, and J. T. Sobczyk, "Recent Developments in Neutrino/ Antineutrino-Nucleus Interactions", Advances in High Energy Physics **2012**, e934597 (2012).

[28]R. E. Taylor, "Deep inelastic scattering: The early years", Reviews of Modern Physics **63**, 573–595 (1991).

[29]C. Andreopoulos et al., "The GENIE neutrino Monte Carlo generator", Nuclear Instruments and Methods in Physics Research Section A: Accelerators, Spectrometers, Detectors and Associated Equipment **614**, 87–104 (2010).

[30]L. Alvarez-Ruso et al., "NuSTEC1 1Neutrino Scattering Theory Experiment Collaboration http://nustec.fnal.gov. White Paper: Status and challenges of neutrino–nucleus scattering", Progress in Particle and Nuclear Physics **100**, 1–68 (2018).

[31]R. Brun and F. Rademakers, "ROOT — An object oriented data analysis framework", Nuclear Instruments and Methods in Physics Research Section A: Accelerators, Spectrometers, Detectors and Associated Equipment, New Computing Techniques in Physics Research V **389**, 81–86 (1997).

[32]C. Andreopoulos et al., *The GENIE Neutrino Monte Carlo Generator: Physics and User Manual*, (Oct. 19, 2015) `http://arxiv.org/abs/1510.05494` (visited on 03/27/2023), preprint.

[33]T. Yang, C. Andreopoulos, H. Gallagher, and P. Kehayias, "A Hadronization Model for the MINOS Experiment", AIP Conference Proceedings **967**, 269–275 (2007).

[34]J. E. Amaro et al., "Neutrino-nucleus scattering in the SuSA model", The European Physical Journal Special Topics **230**, 4321–4338 (2021).

[35]e4 Collaboration et al., "Inclusive electron scattering and the genie neutrino event generator", Physical Review D **103**, 113003 (2021).

[36]B. A. Mecking et al., "The CEBAF large acceptance spectrometer (CLAS)", Nuclear Instruments and Methods in Physics Research Section A: Accelerators, Spectrometers, Detectors and Associated Equipment **503**, 513–553 (2003).

[37]S. T. McLauchlan, "Delta electroproduction in 12C", PhD thesis (University of Glasgow, Scotland, 2003), 145 pp.

[38]V. D. Burkert et al., "The CLAS12 Spectrometer at Jefferson Laboratory", Nuclear Instruments and Methods in Physics Research Section A: Accelerators, Spectrometers, Detectors and Associated Equipment **959**, 163419 (2020).

[39]A. Papadopoulou, *e4nuanalysiscode*, `https://github.com/e4nu/e4nuanalysiscode` (visited on 03/27/2023), github repository.

[40]A. Papadopoulou, *Lepton-Nucleus Scattering Measurements for Neutrino Interactions and Oscillations*, (Jan. 8, 2023) `http://arxiv.org/abs/2301.03114` (visited on 03/26/2023), preprint.

[41]J. Kocka, *SHP_genieanalysis_e4nu*, `https://github.com/kockahonza/SHP_GenieAnalysis_e4nu` (visited on 03/27/2023), github repository.

[42]L. Taling, "Isolation and analysis of 1e1π events from electron-nucleus scattering simulations", MSc Thesis (University of Edinburgh, Scotland, 2022), unpublished.

[43]X.-G. Lu et al., "Measurement of nuclear effects in neutrino interactions with minimal dependence on neutrino energy", Physical Review C **94**, 015503 (2016).

Appendices

A Additional data and plots

π, nucleon	Event set	Uses W cut	QE [%]	Δ_{1232} RES [%]	Other RES [%]	DIS [%]
$1\pi^-1p$	PS	no	0.00	21.13	22.78	56.09
$1\pi^-1p$	PS	yes	0.00	59.36	8.28	32.36
$1\pi^-1p$	FSR	no	0.00	14.30	18.25	67.45
$1\pi^-1p$	FSR	yes	0.00	50.51	6.41	43.08
$1\pi^-1p$	FS	no	0.18	16.49	20.54	62.78
$1\pi^-1p$	FS	yes	0.72	54.21	6.97	38.09
$1\pi^-1p$	DL	no	0.16	15.71	20.52	63.59
$1\pi^-1p$	DL	yes	0.71	54.23	7.15	37.89
$1\pi^+1n$	PS	no	0.00	15.82	31.28	52.90
$1\pi^+1n$	PS	yes	0.00	55.06	17.80	27.14
$1\pi^+1n$	FSR	no	0.00	12.87	26.47	60.66
$1\pi^+1n$	FSR	yes	0.00	49.93	15.34	34.73
$1\pi^+1n$	FS	no	0.20	13.02	27.59	59.19
$1\pi^+1n$	FS	yes	1.00	50.47	15.51	33.02
$1\pi^+1n$	DL	no	0.12	12.06	30.67	57.16
$1\pi^+1n$	DL	yes	0.69	51.53	18.98	28.80

Table 2: Shows how many of each presented type of events there were in each data run for $1\pi^-1p$ and $1\pi^+1n$runs. The percentages are of all passing events from the run so they don't necessarily have to add to 100% if any other unmentioned types occurred, however from these the minimum was 99.987% meaning our select types of events are very close to covering all occurring types.

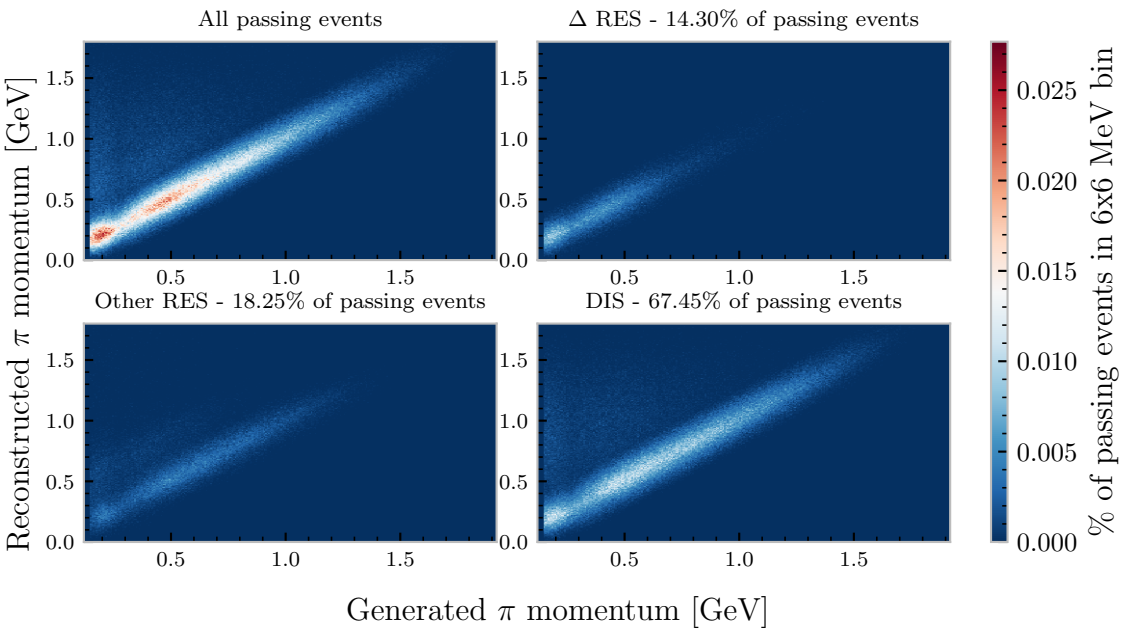

(a) $1\pi^{-}1p$ event set

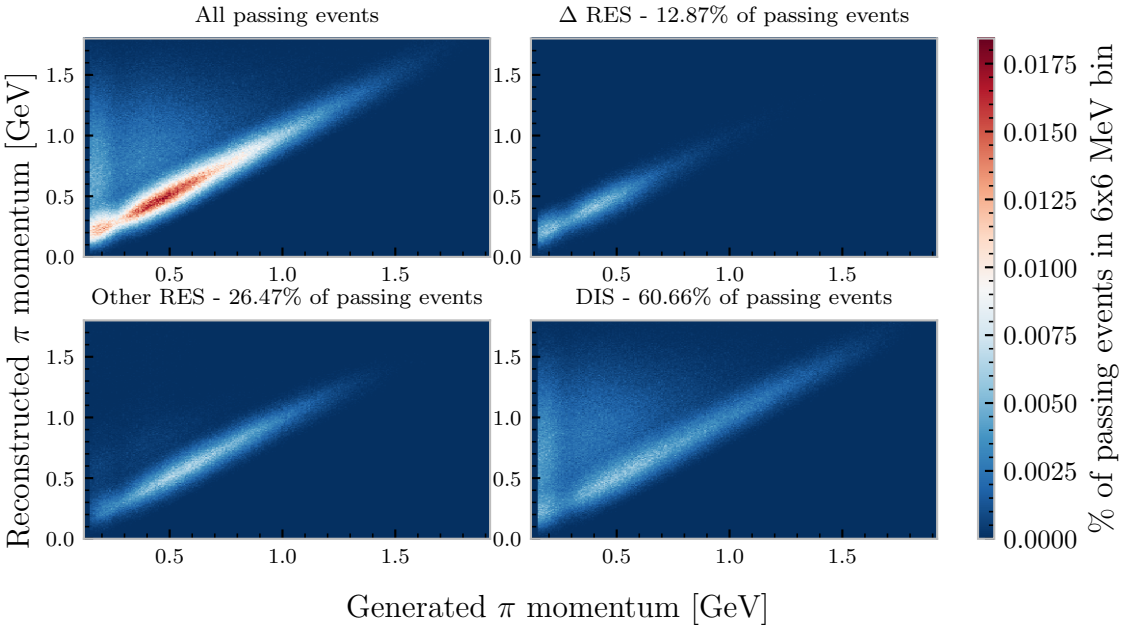

(b) $1\pi^{+}1n$ event set

Figure 17: Correlation of actual and reconstructed pion momentum magnitude for the FSR, no W cut data. Both similar to their counterparts figs. 12 and 13 with a notable difference being a gap at actual pion momentum near 270MeV. This points to FSI being prominent at these momenta as the only difference between PS and FSR event sets is that events with FSI will not be present in FSR. Data to test this specifically however was not collected. Carbon target and 2.26GeV beam energy.

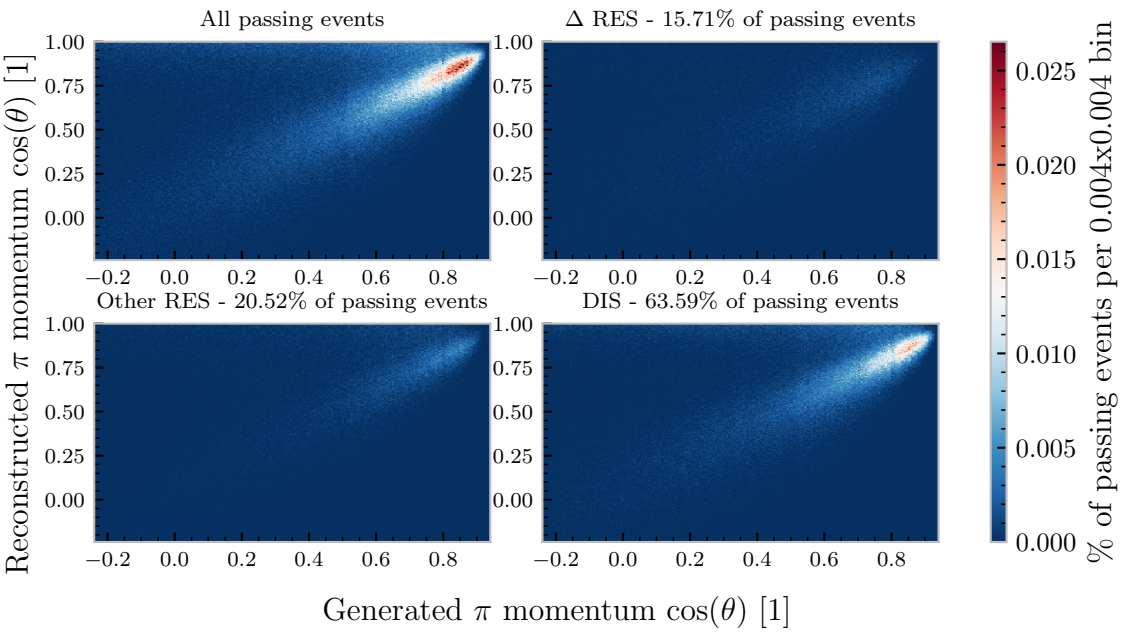

(a) $\cos(\theta)$ reconstruction performance

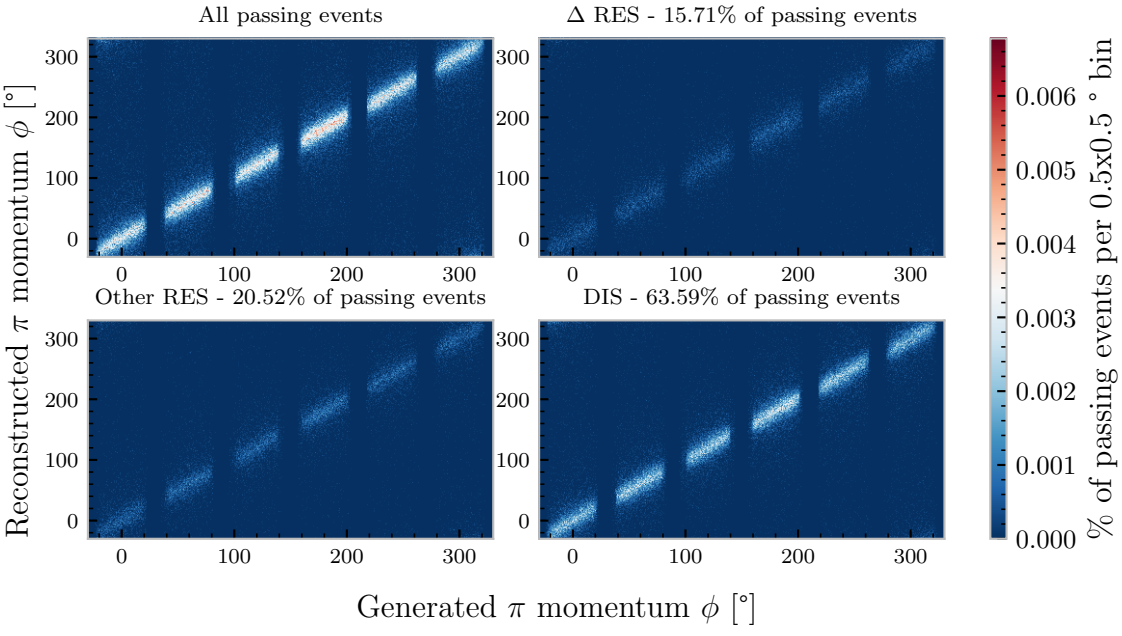

(b) ϕ reconstruction performance

Figure 18: Performance of the directional part of pion 3 momentum reconstruction for the DL, $1\pi^{-}1p$, no W cut data. Other event sets performed very similarly. The ϕ plot clearly shows how only pions passing the fiducials cuts are accepted (showing the 6 sectors from section 3.1). The "flare" going left and slightly up from the dominant cluster of events in the $\cos(\theta)$ is likely due to not true $1\pi^{-}1p$events with undetected particles. Carbon target and 2.26GeV beam energy.

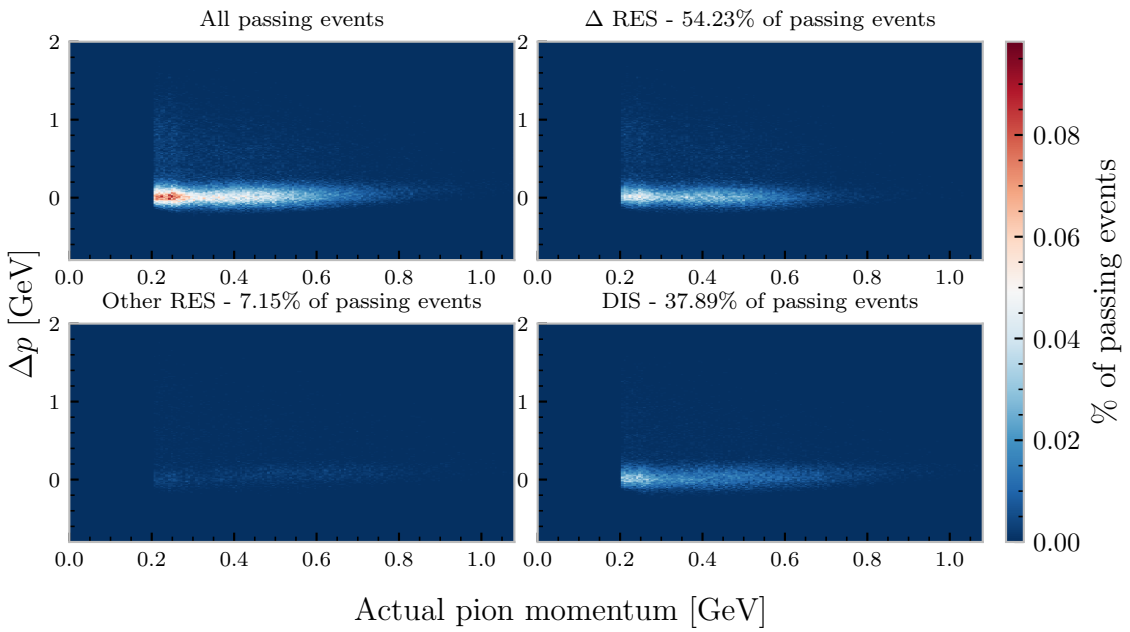

Figure 19: Demonstrating that there is no real correlation between the pion reconstruction performance and the real pions momentum, similar plots for $\cos(\theta)$ and ϕ were also inspected. Possibly the slight tilt of the Other RES data would be worth inspecting. Data for the $1\pi^{-}1p$, DL with W cut, C target and 2.26GeV beam energy.

B A couple more notes on the code

To touch on the project structure, the classes mentioned in section 3.3 and the following ones are implemented in the `GenieAnalysis` folder, then there are executables, these are `.cpp` files in the root folder which specify a given run. For the other, see fig. 20, the `GACLAS6Common` file (and namespace) defines specific properties specific to the CLAS6 data (like target and beam energy enums) and a wrapper around the original fiducials code. The `GACLAS6MCCuts, GACLAS6MC` classes do equivalent analysis to that which the original code (as inherited from Taling[42]) did on the GENIE data for CLAS6. This was mainly used for first looks and testing of the new code (having five executables using these) and `GACLAS6DataPrepare, GACLAS6Data` do the equivalent for the actual CLAS6 data, though this has not been tested much.

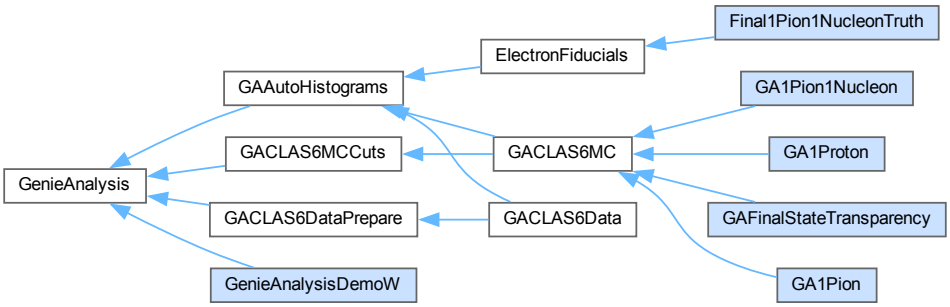

Figure 20: A class diagram of the new code showing the relations. The reusable classes from the `GenieAnalysis` folder are shown with a white background, classes from executables are light blue.